Oxygen vacancy ordering in heavily rare-earth-doped ceria

Ding Rong Ou, Toshiyuki Mori, Fei Ye, Tomoaki Kobayashi, Jin Zou, Graeme Auchterlonie, and John Drennan

Citation: Applied Physics Letters **89**, 171911 (2006); doi: 10.1063/1.2369881

View online: http://dx.doi.org/10.1063/1.2369881

View Table of Contents: http://scitation.aip.org/content/aip/journal/apl/89/17?ver=pdfcov

Published by the AIP Publishing

Oxygen vacancy ordering in heavily rare-earth-doped ceria

Ding Rong Ou,[a] Toshiyuki Mori, Fei Ye, and Tomoaki Kobayashi
Fuel Cell Materials Center, National Institute for Materials Science, 1-1 Namiki, Tsukuba, Ibaraki 305-0044, Japan

Jin Zou
School of Engineering, The University of Queensland, St. Lucia, Queensland 4072, Australia and Centre for Microscopy and Microanalysis, The University of Queensland, St. Lucia, Queensland 4072, Australia

Graeme Auchterlonie and John Drennan
Centre for Microscopy and Microanalysis, The University of Queensland, St. Lucia, Queensland 4072, Australia

(Received 1 September 2006; accepted 14 September 2006; published online 26 October 2006)

25 at. % Rare-earth (RE)-doped ceria samples (RE=Sm, Dy, Y, and Yb) were examined using transmission electron microscopy and electron energy loss spectroscopy, from which the oxygen vacancy ordering in nanosized domains was confirmed. The relationships of the dopant type, oxygen vacancy ordering, and ionic conductivity of doped ceria were established. It is found that the ordering of oxygen vacancies depends strongly on the dopant type, and the development of nanosized domains with a higher degree of ordering can lead to a more dramatic decrease of ionic conductivity in doped ceria. © *2006 American Institute of Physics*. [DOI: 10.1063/1.2369881]

Rare-earth (RE)-doped ceria with cubic fluorite structure is an important ionic conductor, which has relatively high ionic conductivity and can be used as an electrolytic material in intermediate temperature solid oxide fuel cells.[1–4] It has been demonstrated that the electrical properties of doped ceria can be significantly influenced by the dopant type. For example, there exists an *optimum radius* of the dopant for the ionic conduction. With the dopant radius deviating from this optimum value, the conductivity of doped ceria decreases dramatically.[2–4] This phenomenon has been attributed to the dopant-oxygen vacancy association that depends on the dopant radius.[2,5–7]

In the dilute doping range, the ionic conduction is dominated by this association between dopant cations and oxygen vacancies and exhibits a maximum conductivity for ceria doped with Sm or Gd because these dopant cations have the optimum radius and, thereby, a smaller association enthalpy.[2–4] However, in heavily doped ceria, nanosized domains can form and impact the ionic conductivity.[8–11] As a consequence, the advantage of the dopant with optimum radius disappears with increasing doping concentration. As shown in a comparative study of Gd- and Y-doped ceria,[12] conductivities in orders of Gd>Y and Gd<Y were observed at doping concentrations lower and higher, respectively, than 20–25 at. %. Zhang *et al.*[12] suggested that it is because the ionic conduction in heavily doped ceria is dominated by the formation of nanosized domains instead of dominated by the association. Although the crystal structure of nanosized domains remains unclear, it has been suspected that the negative impacts of domains on ionic conduction are related to its ordered structure, which is different from the fluorite-structured matrix, and possibly involve some ordering of oxygen vacancies.[11,12]

In this letter, in order to explore the ordered structure in nanosized domains, transmission electron microscopy (TEM) and electron energy loss spectroscopy (EELS) were performed on heavily doped ceria as EELS can be used to detect the oxygen vacancy ordering in oxides.[13,14] Based on the EELS study, the oxygen vacancy ordering in ceria doped with different RE elements is evaluated. Then the dependence of the ordering on the dopant type and its influence on electrical properties are discussed.

Round and well-dispersed nanopowders of pure ceria (CeO_2) and RE-doped ceria (RE=Sm, Dy, Y, and Yb) were synthesized using the ammonium carbonate coprecipitation method.[11] From the nanopowders, highly dense samples were obtained through sintering at 1400–1450 °C for 6 h. The microstructure of sintered samples was examined by selected area electron diffraction (SAED) and high resolution transmission electron microscopy (HRTEM) using a JEM-2000EX TEM. EELS and energy-filtered transmission electron microscopy (EFTEM) were performed using a FEI Tecnai-F30 TEM equipped with a Gatan imaging filtering system. The TEM specimens were prepared by mechanical polishing and dimpling, followed by ion milling.

Through extensive HRTEM and EFTEM investigations, nanosized domains were observed in 25 at. % RE-doped ceria. No obvious difference in size and density of domains was observed between samples with different dopants. Figure 1(a) is an example and shows elemental maps of 25 at. % Y-doped ceria obtained by EFTEM, on which nanosized domains rich in dopant cations but poor in Ce can be clearly seen. As a result of the formation of the domains, SAED studies showed diffuse scattering and/or extra spots superimposed with the diffraction spots of the fluorite matrix. Apparently, this is due to the superlattice formed in the nanosized domains. Figures 1(b)–1(e) are [110] SAED patterns of ceria doped with Sm, Dy, Y, and Yb. In the case of Sm- and Dy-doped ceria, the extra spots (some marked by arrows) are readily visible [Figs. 1(b) and 1(c)]. However, these extra spots become faint and then almost disappear as the dopant is switched to Y [Fig. 1(d)] and Yb [Fig. 1(e)]. Inversely, the

[a]Electronic mail: dingrong.ou@nims.go.jp

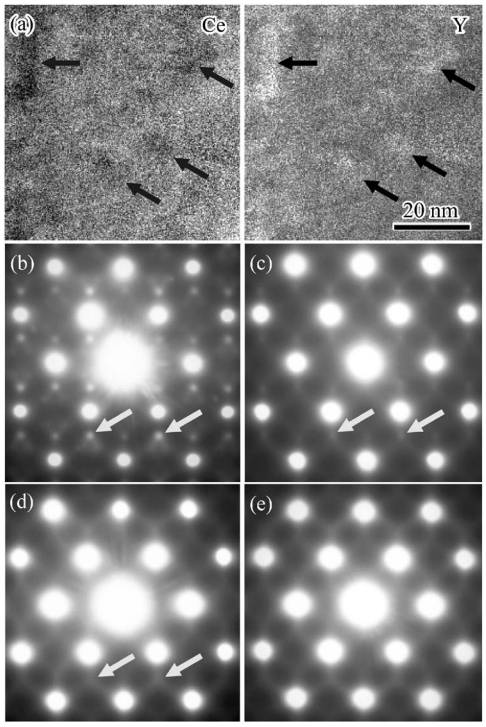

FIG. 1. (a) Ce and Y maps of Y-doped ceria and SAED patterns of ceria doped with (b) Sm, (c) Dy, (d) Y, and (e) Yb.

diffuse scattering between the diffraction spots becomes stronger with the disappearance of extra spots, indicating that the ordered structure in domains is strongly dependent on the dopant type. Obviously, the domains in Sm-doped ceria have a more ordered structure than those in other doped ceria.

To determine oxygen vacancy ordering in nanosized domains, an EELS investigation was carried out. Figure 2 shows the oxygen *K* edges for the pure ceria and 25 at. % RE-doped ceria, in which backgrounds have been removed. Three characteristic peaks (marked by A, B, and C) can be clearly distinguished. Among these characteristics, peak A is obvious in pure ceria but weaker in doped ceria, which could be explained by the decrease of Ce concentration in doped ceria since this preedge peak is related to the hybridization between oxygen and Ce^{4+} cations.[15,16] Inversely, the relative intensity of peak B in doped ceria is considerably higher than

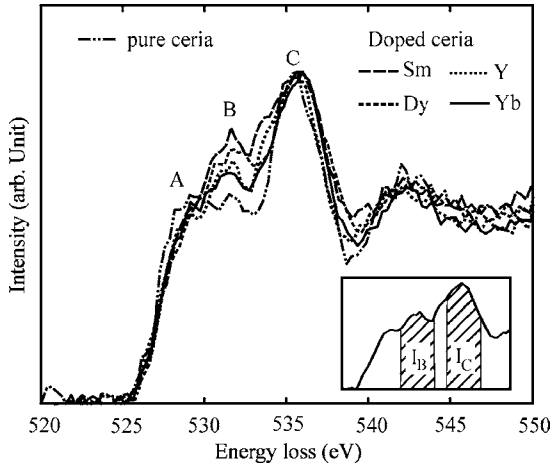

FIG. 2. Oxygen *K*-edge of pure ceria and 25 at. % RE-doped ceria samples. Inset shows the energy windows with a width of 2 eV for calculating the integral intensities of peaks B and C.

TABLE I. Comparison between the value of $\Delta(I_B/I_C)$ and the ionic conductivity (in air) of 15 and 25 at. % RE-doped ceria ($\sigma 15$ and $\sigma 25$).

		Ionic conductivity at 500 °C (S/cm)		
Dopant	$\Delta(I_B/I_C)$	$\log \sigma_{15}$	$\log \sigma_{25}$	$\log \sigma_{15}$-$\log \sigma_{25}$
Sm	0.17	−2.28	−2.89	0.61
Dy	0.13	−2.42	−2.78	0.36
Y	0.08	−2.41	−2.72	0.31
Yb	0.07	−2.74	−2.93	0.19

that of pure ceria. Previous studies had shown that the intensities of peaks B and C can be influenced by the crystal structure[16,17] and particularly, the enhancement of peak B could be introduced by the ordering of oxygen vacancies in nonstoichiometric oxides.[14] In our samples, the increase in peak B is different with a sequence of Sm > Dy > Y > Yb, which agrees with the extra diffraction spots on SAED patterns (Fig. 1). Therefore, we believe that the observed enhancement of peak B in this study is also related to the oxygen vacancy ordering in nanosized domains. Such ordering might be a product of the segregation of dopant cations and thereby the enrichment of oxygen vacancies in the domains.

In our previous work, it has been demonstrated that the nanodomains could have negative impact on the ionic conductivity of doped ceria.[11] Based on the EFTEM investigation shown in Fig. 1, we believe that this phenomenon is related to the interaction between the oxygen vacancies and the segregated dopant cations, and, probably, such impact could be enhanced by the oxygen vacancy ordering in the domains. For the purpose of comparison, the increase in peak B, whose value could be related to the degree of the oxygen vacancy ordering, was calculated as $\Delta(I_B/I_C)=(I_B/I_C)-(I_B/I_C)_{CeO_2}$, where I_B and I_C are the integral intensities of peaks B and C calculated using energy windows with a width of 2 eV (as illustrated by the insert in Fig. 2). Here we used pure ceria as a standard sample for comparison since the calculated value of I_B/I_C for pure ceria (~0.65) is very close to the ratio of 2/3 for CeO_2 with an ideal fluorite structure (calculated from the band density of states).[16] Table I displays both the value of $\Delta(I_B/I_C)$ and the conductivity of doped ceria measured at 500 °C (in air) by the dc three-probe method. As the doping concentration becomes 15 at. %, the amount of nanosized domains is too small to impact the conductivity,[8–11] so that the conduction is dominated by the association enthalpy and shows a maximum conductivity in Sm-doped ceria. This tendency agrees with other studies.[2–4] With the increase of the doping concentration to 25 at. %, nanosized domains can be developed, which, in turn, decrease the conductivity.[10,11] Table I shows not only the decrease in conductivity with the increasing doping concentration, but also the fact that such decrease can be speeded up with increasing $\Delta(I_B/I_C)$, indicating that the ionic conduction in heavily doped ceria is dominated by the formation of nanosized domains and that the domains with a higher degree of ordering can block the oxygen vacancies more effectively.

It is of interest to note that, although the domain formation is related with the association between oxygen vacancies and segregated dopant cations,[11,18] this study shows that the degree of oxygen vacancy ordering in nanosized domains is in an order inverse to that of the association (Sm < Dy < Y

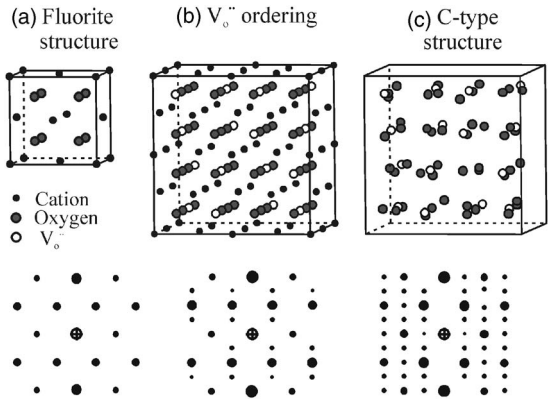

FIG. 3. Schematic of constructing a unit cell of a *C*-type structure out of eight unit cells of fluorite structure by removing 25% oxygen ions [(a) →(b)] and then introducing ionic shifts [(b)→(c)]. Corresponding [110] electron diffraction patterns are shown. To clearly present the arrangement of oxygen ions in a *C*-type structure, the shifted cations in (c) are hidden.

<Yb).[2,5–7] A possible reason for this controversy is that the association between dopant cations and oxygen vacancies is an interaction at the atomic level, while the formation of the ordered structure can be influenced by other factors in a longer range. To clarify this point, the understanding of the ordered structure in domains is required. Since a solid solution of Ce in *C*-type RE_2O_3 can form in a CeO_2–$REO_{1.5}$ system at a higher doping concentration (>33%–40%),[19,20] we believe that the formation of nanosized domains with higher dopant concentration than their matrix could be a symptom of a transition from the fluorite ceria to *C*-type RE_2O_3, and the oxygen vacancy ordering in these domains could have a structure between fluorite and *C*-type structures. As shown in Fig. 3, a unit cell of *C*-type structure can be constructed out of eight unit cells of fluorite structure by removing 25% of oxygen ions with introducing ionic shifts. During this process, the oxygen vacancy ordering based on the fluorite structure could be geometrically formed [Fig. 3(b)], and the corresponding electron diffraction pattern (simulated using the software CARINE CRYSTALLOGRAPHY 3.1) is rather close to the obtained SAED patterns (Fig. 1). Therefore, it is possible that part of the associated oxygen vacancies in nanosized domains can be further arranged in a superstructure similar to that in Fig. 3(b) in order to stabilize the existence of domains.

Since the structure of domains can be approximately described between ceria and *C*-type RE_2O_3, a higher degree of ordering indicates that the domains have a structure closer to the *C*-type structure. For this reason, we suspect that one influencing factor for the forming ability of oxygen vacancy ordering in the domains could be the lattice difference between the fluorite-structured ceria and *C*-type RE_2O_3. Thus, the mismatch between the lattice parameters of CeO_2 and *C*-type RE_2O_3 was calculated as $\Delta a=(1/2a_C-a_F)/a_F$, where a_F and a_C are lattice parameters of fluorite-structured CeO_2 and *C*-type RE_2O_3.[21] Figure 4 presented the values of $\Delta(I_B/I_C)$ as a function of Δa. It is clearly shown that a smaller value of Δa can lead to a higher degree of oxygen vacancy ordering in nanosized domains.

In conclusion, TEM and EELS studies have confirmed the oxygen vacancy ordering in nanosized domains in heavily RE-doped ceria (RE=Sm, Dy, Y, and Yb). The relationship between dopant type, oxygen vacancy ordering, and ionic conductivity has been established: (1) the oxygen vacancy ordering depends strongly on dopant type in a sequence of Sm>Dy>Y>Yb, which can be explained in terms of the difference in the lattice parameters between fluorite-structured ceria and *C*-type dopant oxides and (2) the development of domains with a higher degree of ordering can lead to a more dramatic decrease in the ionic conductivity of doped ceria.

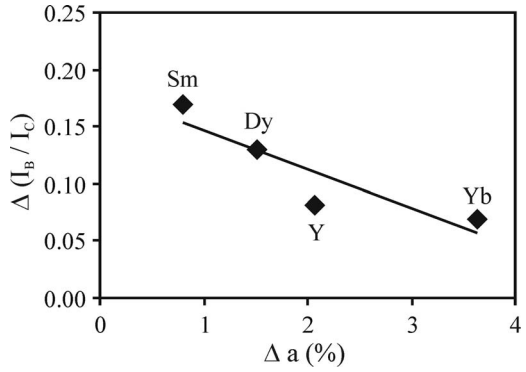

FIG. 4. Values of $\Delta(I_B/I_C)$ as a function of the difference in lattice parameters of *C*-type RE_2O_3 and fluorite-structured ceria (Δa).

The financial support from the Grant-in-Aid for Scientific Research on Priority Area, Nanoionics (439) by the Ministry of Education, Culture, Sports, and Technology, Japan and from the Australian Research Council are acknowledged.

[1] B. C. H. Steele and A. Heinezl, Nature (London) **414**, 345 (2001).
[2] H. Inaba and H. Tagawa, Solid State Ionics **83**, 1 (1996).
[3] G. B. Balazs and R. S. Glass, Solid State Ionics **76**, 155 (1995).
[4] K. Eguchi, T. Setoguchi, Y. Inoue, and H. Arai, Solid State Ionics **52**, 165 (1992).
[5] E. C. Subbarao and H. S. Maiti, Solid State Ionics **11**, 317 (1984).
[6] V. Bulter, C. R. A. Catlow, B. E. F. Fender, and J. H. Harding, Solid State Ionics **8**, 109 (1983).
[7] R. Gerhardt-Anderson and A. S. Nowick, Solid State Ionics **5**, 547 (1981).
[8] T. Mori, J. Drennan, J.-H. Lee, J.-G. Li, and T. Ikegami, Solid State Ionics **154–155**, 461 (2002).
[9] T. Mori, Y. Wang, J. Drennan, G. Auchterlonie, J.-G. Li, and T. Ikegami, Solid State Ionics **175**, 641 (2004).
[10] T. Mori, J. Drennan, Y. Wang, G. Auchterlonie, J.-G. Li, and A. Yago, Sci. Technol. Adv. Mater. **4**, 213 (2003).
[11] D. R. Ou, T. Mori, F. Ye, M. Takahashi, J. Zou, and J. Drennan, Acta Mater. **54**, 3737 (2006).
[12] T. S. Zhang, J. Ma, L. B. Kong, S. H. Chan, and J. A. Kilner, Solid State Ionics **170**, 209 (2004).
[13] R. F. Klie, Y. Ito, S. Stemmer, and N. D. Browning, Ultramicroscopy **86**, 289 (2001).
[14] A. Travlos, N. Boukos, G. Apostolopoulos, and A. Dimoulas, Appl. Phys. Lett. **82**, 4053 (2003).
[15] R. C. Karnatak, J. Alloys Compd. **192**, 64 (1993).
[16] A. V. Soldatov, T. S. Ivanchenko, S. Della Longa, A. Kotani, Y. Iwamoto, and A. Bianconi, Phys. Rev. B **50**, 5074 (1994).
[17] L. Douillard, M. Gautier, N. Thromat, M. Henriot, M. J. Guitter, J. P. Duraud, and G. Tourillon, Phys. Rev. B **49**, 16171 (1994).
[18] D. R. Ou, T. Mori, F. Ye, J. Zou, G. Auchterlonie and J. Drennan, Electrochem. Solid-State Lett. (in press).
[19] V. Longo and L. Podda, J. Mater. Sci. **16**, 839 (1981).
[20] S. V. Chavan, M. D. Mathews, and A. K. Tyagi, J. Am. Ceram. Soc. **87**, 1977 (2004).
[21] JCPDS-International Center for Diffraction Data, Card No. 43-1002, Card No. 43-1006, Card No. 43-1029, Card No. 43-1036, Card No. 43-1037.